


Circular RNA expression profiles in extracellular vesicles from the plasma of patients with pancreatic ductal adenocarcinoma

Qingqing Li^{1,2} , Shasha Geng², Huixiao Yuan², Yang Li², Shuxian Zhang^{1,3}, Lin Pu², Jianli Ge², Xianping Niu², Yandong Li⁴ and Hua Jiang^{1,2}

1 Shanghai East Hospital, Nanjing Medical University, Shanghai, China

2 Department of Geriatrics, Shanghai East Hospital, Tongji University School of Medicine, Shanghai, China

3 Department of Gastroenterology, The First People's Hospital of Lianyungang, China

4 Research Center for Translational Medicine, Shanghai East Hospital, Tongji University School of Medicine, Shanghai, China

Keywords

circular RNA; extracellular vesicles; microRNA; pancreatic ductal adenocarcinoma

Correspondence

H. Jiang, Department of Geriatrics, Shanghai East Hospital, Tongji University School of Medicine, 150 Jimo Road, Shanghai 200120, China
Fax: +86 021 58873265
Tel: +86 021 58873265
E-mail: huajiang2013@tongji.edu.cn
and

Y. Li, Department of Oncology, Shanghai East Hospital, Tongji University School of Medicine, 150 Jimo Road, Shanghai 200120, China
Fax: +86 21 58798999
Tel: +86 21 61569884
E-mail: yandongli2009@gmail.com

Qingqing Li and Shasha Geng contributed equally to this article

(Received 18 June 2019, revised 26 September 2019, accepted 9 October 2019)

doi:10.1002/2211-5463.12741

Tumor-derived extracellular vesicles (EVs) and their contents are involved in the development of human malignancies. Circular RNAs (circRNAs), enriched in EVs, can regulate diverse cellular processes by acting as microRNA (miRNA) sponges or through other mechanisms. In the present study, we explored the potential roles of circRNAs in EVs in the development of pancreatic ductal adenocarcinoma (PDAC). First, plasma was obtained from patients with PDAC ($n = 8$) and healthy volunteers ($n = 8$), and EVs were isolated by the ultracentrifugation method. Nanoparticle tracking analysis and transmission electron microscopy confirmed the size and form of the isolated EVs. The circRNA expression profiles of EVs were investigated by high-throughput whole transcriptome sequencing. We then further validated the accuracy of the circRNA sequencing data by quantitative real-time PCR analysis using plasma samples and PC cell lines, and subsequently performed bioinformatics analysis to reveal the potential functional roles of the differentially expressed circRNAs and to construct a circRNA-miRNA interaction network to predict the target miRNAs of these circRNAs. Our work provides novel targets for further studies concerning the pathogenesis of PDAC.

Pancreatic ductal adenocarcinoma (PDAC) is the fourth leading cause of cancer-related death in the United States, with an estimated 45 750 deaths of this disease in 2019 [1]. Late diagnostic capabilities, early metastasis

and a fast developing chemoresistance lead to a poor prognosis of patients with PDAC, with a 5-year survival rate of less than 5% [2]. Therefore, a better understanding of the molecular mechanisms behind the

Abbreviations

BP, biological process; CC, cellular component; circRNA, circular RNA; circRNA-seq, circular RNA sequencing; EV, extracellular vesicle; GO, Gene Ontology; KEGG, Kyoto Encyclopedia of Genes and Genomes; MF, molecular function; miRNA, microRNA; NTA, nanoparticle tracking analysis; PDAC, pancreatic ductal adenocarcinoma; RNA-seq, RNA sequencing; TEM, transmission electron microscope.

carcinogenesis and development of PDAC is essential for developing effective therapies against PDAC.

Extracellular vesicles (EVs) are 30- to 120-nm phospholipid bilayer-enclosed membrane nanoparticles that are released from various types of cell and are found in abundance in body fluids including blood, saliva, urine and breast milk [3–5]. The components of EVs vary according to different cell types and mechanism of biogenesis, including lipid, proteins, mRNAs, DNA fragments and noncoding RNAs [6–9]. Accumulating evidence has indicated that EVs are essential for intercellular communication and participate in many physiological and pathological processes [10–12], and importantly, EVs derived from tumor cells have been found to play key roles in the development of human malignancies by transferring their components into target cells to regulate tumor initiation, tumor cell growth, metastasis, immune response, systemic cell-to-cell relevance and so on [13,14]. For instance, Melo *et al.* [15] found GPC1⁺ circulating exosomes were highly expressed in the serum of patients with pancreatic cancer and correlated with tumor burden, exosome-mediated transfer of miR-10b was reported to promote cell invasion of breast cancer [16]. Among the components of exosomes, circular RNAs (circRNAs) are a novel type of noncoding RNA, which is becoming a hot spot in cancer research [17–19]. Unlike linear RNAs terminated with 5' caps and 3' tails, circRNAs form covalently closed continuous loop structures [20]. They could act as microRNA (miRNA) sponges, regulators of splicing and transcription and modifiers of parental gene expression [20–22]. In recent years, scientists have proved that circRNAs participate in some pathological process, such as prion infection [23], neurological disorders [24] and atherosclerotic vascular disease [25], and especially in various human malignancies [26–28]. In 2015, Li *et al.* [29] first identified more than 1000 circRNAs in human serum exosomes and revealed that circRNAs were enriched in exosomes of liver cancer cells compared with the producer cells by RNA sequencing (RNA-seq) analyses. A previously identified circRNA, ciRS-7, could promote epidermal growth factor receptor expression by acting as a miRNA sponge of miR-7, and epidermal growth factor receptor overexpression was related to tumor progression and resistance to chemotherapy [21,30]. However, due to the numerous types of pancreatic cancer-derived EV and diverse contents, little is known about EVs circRNAs in PDAC, and using them as potential biomarkers of PDAC is still at an exploratory stage.

In this study, EVs from plasma of patients with PDAC and healthy volunteers were isolated and

characterized first, after which we evaluated the EVs circRNA expression profiles in PDAC ($n = 8$) and normal plasma samples ($n = 8$) by high-throughput whole transcriptome sequencing. Furthermore, bioinformatic analysis was used to predict the function of differentially expressed circRNAs, and 13 differentially expressed circRNAs were selected to validate the accuracy of the RNA-seq data by quantitative real-time PCR analysis. In addition, a circRNA–miRNA interaction network was constructed. Our work could provide a basis for further studies concerning the functions of EVs circRNAs in PDAC.

Materials and methods

Sample collection

Blood samples (8 mL) from eight patients with PDAC and eight healthy volunteers were collected in Shanghai East Hospital from May 2017 to March 2018. All of the patients with PDAC were diagnosed according to the seventh edition of the *American Joint Committee on Cancer* staging manual and confirmed by pathologists after surgery, and they accepted neither radiotherapy nor chemotherapy before surgery. Fasting venous blood was drawn and centrifuged; the separated plasma was stored at -80°C before the experiments. This study was approved by the Ethics Committee of Biomedicine Research at Shanghai East Hospital, Tongji University, and written informed consent was obtained from each participant in this study. The use of patient samples conformed to the guidelines set by the Declaration of Helsinki.

Extraction and characterization of the PDAC-derived EVs

The plasma samples were centrifuged at 1500 *g* for 5 min and then 10 000 *g* for 30 min at 4°C , after which the debris was removed. Supernatant was filtered through a 0.22- μm filter to remove large particles and then centrifuged at 150 000 *g* for 16 h to obtain the EVs. The pellet containing EVs was diluted with PBS and centrifuged at 150 000 *g* for 2 h. EVs were purified by density gradient ultracentrifugation, then stored at -80°C before quantitation. All ultracentrifugation steps were performed in an Optima L-100XP ultracentrifuge (Beckman Coulter, Brea, CA, USA). The EV samples were diluted with PBS (1 : 100) before diameter and concentration quantitation, and a NanoSight NS300 instrument (Malvern Instruments, Malvern, UK) was used for nanoparticle tracking analysis (NTA). Each sample was read in triplicate. The size and number of the vesicles were recorded by the NTA software (NanoSight Limited, Malvern Instruments, Amesbury, UK).

Transmission electron microscopy

EVs were visualized using a transmission electron microscope (TEM) (JEM-2100F; JEOL, Tokyo, Japan). In brief, samples for TEM were diluted to 1 mg·mL⁻¹ in PBS and absorbed onto carbon/formvar TEM grids (400 mesh). After drying for 10 min at room temperature, the grids were stained with phosphotungstic acid solution (2%, pH 7.0) for 15 min. After further drying overnight at room temperature, the stained grids were observed and photographed using a TEM.

RNA library construction and circRNA sequencing

For total RNA extraction from EVs, TRIzol reagent (Invitrogen, Carlsbad, CA, USA) was used according to the manufacturer's instruction. The concentration and purity of each RNA sample were measured by NanoDrop ND-1000 (Thermo Fisher Scientific, Waltham, MA, USA). Standard denaturing agarose gel electrophoresis was used to examine RNA integrity. RNA library construction and circRNA sequencing (circRNA-seq) were performed by CloudSeq Biotech Inc. (Shanghai, China). To enrich circRNAs and deplete rRNAs, we treated the total RNA with RNase R (Epicentre, Madison, WI, USA) and the Ribo-Zero Magnetic Gold Kit (Epicentre). RNA libraries were constructed using the rRNA-depleted RNAs with TruSeq Stranded Total RNA Library Prep Kit (Illumina, San Diego, CA, USA) according to the manufacturer's protocols. The BioAnalyzer 2100 system (Agilent Technologies, Santa Clara, CA, USA) was used to confirm the quality and quantity of the libraries. Libraries were denatured into single-stranded DNA molecules, captured on Illumina Flow Cells (Illumina) and then amplified *in situ* as clusters, and finally sequenced for 150 cycles using the HiSeq 4000 Sequencing system (Illumina).

Bioinformatics analysis

Gene Ontology (GO) (<http://www.geneontology.org>) and Kyoto Encyclopedia of Genes and Genomes (KEGG) pathway analyses (<http://www.genome.jp/kegg>) were performed for the differentially expressed circRNA-associated genes. The coordinates of the mRNA (which is defined as the circRNA-associated gene) were predicted through the RefSeq database based on back-splicing site coordinates of the circRNA. The circRNA-miRNA network was generated by CYTOSCAPE software (<http://www.cytoscape.org/download.html>).

Quantitative real-time PCR analysis

Quantitative real-time PCR analysis was performed to verify the accuracy of the circRNA-seq data. The target RNA and internal parameters of each sample were respectively

subjected to quantitative real-time PCRs on an Applied Biosystems 7500 Fast qRT-PCR System (software version 2.0.5; Roche, Basel, Switzerland). Total RNA was reverse transcribed to synthesize cDNA using a Prime Script RT Reagent Kit (Perfect Real Time; TaKaRa, Osaka, Japan). The data were analyzed by the 2^{-ΔΔC_T} method. An outward-facing primer was typically designed for an exon sequence near the back-splice site (within 150 nucleotides up or down) of the corresponding circRNA. Primers of the selected circRNAs and internal parameters of GAPDH were shown in Table 1. Thirteen differentially expressed circRNAs were used in experimental validation including eight up-regulated circRNAs and five down-regulated circRNAs. Moreover, expression of four up-regulated circRNAs was detected in pancreatic cancer cells.

Cell culture

Human pancreatic cancer cells (BxPC-3, COLO-357, PANC-1 and SW1990) were purchased from the American Type Culture Collection (ATCC, Manassas, VA, USA). BxPC-3 cells were cultured in RPMI 1640 medium (Corning, NY, USA) supplemented with 10% fetal bovine serum

Table 1. Primers used for quantitative real-time PCR analysis of circRNA levels. F, forward; PS, product size; R, reverse.

Target ID	Primer sequence (5'-3')	PS (bp)
hsa_circ_0002130	F: CCACGTGGGAGATTCTGG R: ACGTTCCACAGCCAGCTC	121
hsa_circ_0000896	F: TCCTGGAGATGGGGTTCA R: GCCAAGAGCCACTGGAGA	233
hsa_circ_0101692	F: TACTCGGCCAGCGTTTA R: TCCATTTCCCGATAGCA	61
hsa_circ_0005882	F: GCCCACCAATGCTAATG R: TGACCACTTGACCCAGGAA	214
hsa_circ_0001250	F: GACAGCGAGGAGCTGAGG R: CCTAACATGACGCTCGGG	167
hsa_circ_0037096	F: GGCAAAGAGGTTGCTGGA R: TGTGAGATGGAGGTGCGA	263
hsa_circ_0000128	F: ATAACAGTTGCTGCCGCC R: TTTCTTTCTTTCCCGGC	163
hsa_circ_0000606	F: ATTGCATTCCAACAGCTCA R: CCGGCCATCAACAATTTT	60
hsa_circ_0103896	F: CCTGAACAGCCAGTGGAGA R: TCCTGGAGGAGGGTTTC	174
hsa_circ_0006662	F: TGGAAAAGAGCCGAGTGG R: CTGCAACCTTTCTCCAGA	190
hsa_circ_0092763	F: GCAGTATGCTGTGGAGGGA R: GGATAGCCTTCAATGAGCCA	215
hsa_circ_0035432	F: GGCCCTGAGGGAGAGTGT R: AGGAGCCTGCCTTGGAGT	167
hsa_circ_0094190	F: GGGCTGTCATCTGGTTGG R: CGATGCACTGCCACCTTA	197
GAPDH	F: GGCCTCAAGGAGTAAGACC R: AGGGGAGATTCAAGTGTGGT	122

(Corning) and 100 U·mL⁻¹ penicillin and streptomycin (Gibco, Grand Island, NY, USA), Colo-357 cells were cultured in RPMI 1640 medium (Corning) supplemented with 20% fetal bovine serum (Corning) and 100 U·mL⁻¹ penicillin and streptomycin (Gibco), and PANC-1 and SW1990 cells were cultured in DMEM medium (Corning) supplemented with 10% fetal bovine serum (Corning) and 100 U·mL⁻¹ penicillin and streptomycin (Gibco). All cell lines were incubated at 37 °C with 5% CO₂. Medium was replaced every other day. At 80% confluence, adhered cells were digested with 0.25% trypsin.

Statistical analysis

For statistical analysis, each experiment was repeated at least three times independently. Data were presented as the mean ± standard deviation. A two-tailed Student's *t*-test was used to assess the difference between two groups. A *P*-value <0.05 was considered statistically significant. All analyses were carried out using SPSS 19.0 software (SPSS, San Rafael, CA, USA).

Results

Detection and characterization of circulating EVs

As mentioned earlier, circulating EVs were isolated from the plasma of patients with PDAC and healthy volunteers, respectively. The vesicles we obtained were examined by NanoSight NTA and TEM analyses to confirm the purification of EVs (Fig. 1). The results of NTA analysis showed that the diameter of the vesicles ranged from 30 to 140 nm, which is in line with the size of EVs (Fig. 1A). In agreement with the previously reported form of EVs, the isolated vesicles displayed a homogeneous population of clearly defined spherical vesicles under TEM (Fig. 1B), hinting that EVs were successfully purified from the plasma samples of patients with PDAC and healthy volunteers.

Differential expression of circRNAs in EVs from the plasma of patients with PDAC

circRNAs in EV samples from plasma of eight patients with PDAC and eight normal healthy volunteers were sequenced, and the circRNA-seq reads of each sample are shown in Table 2. A total of 453 significantly differentially expressed circRNAs were finally identified using the criteria of fold change ≥ 2.0 and *P* ≤ 0.05. Among these circRNAs, 274 were up-regulated and 179 were down-regulated. Hierarchical clustering analysis was subsequently performed to illustrate the distinguishable circRNA expression profile of the samples. As shown in Fig. 2A, the circRNAs exhibited

a different expression pattern in patients with PDAC compared with the control group. According to the means of the expression values of the samples from two groups, a scatterplot was drawn to illustrate the variation of circRNA expression of the two groups (Fig. 2B). Furthermore, differentially expressed circRNAs with statistical significance (fold change > 2.0, *P* < 0.05) between the two groups were identified and filtered using a volcano plot (Fig. 2C), and the dysregulated circRNAs were summarized and classified on the basis of their categories. Among the up-regulated circRNAs, there are 3 antisense, 232 exonic, 9 intronic, 24 sense overlapping and 6 intragenic (Fig. 2D). Among the down-regulated circRNAs, there are 18 antisense, 25 exonic, 48 intronic, 69 sense overlapping and 19 intragenic (Fig. 2E).

Bioinformatics analysis of the differentially expressed circRNAs

circRNA-derived genes were subjected to GO analysis to annotate and speculate the functional roles of the differentially expressed circRNAs in terms of biological processes (BPs), cellular components (CCs) and molecular functions (Fig. 3). GO analysis of BPs showed that the differentially expressed circRNAs were significantly associated with positive regulation of BP, organelle organization, positive regulation of metabolic progress, epidermis development, cell-type-specific apoptotic process and Purkinje cell differentiation. In regard to CC, these circRNAs exhibited a strong relationship with intracellular part, organelle part, intracellular, basolateral plasma membrane, sperm midpiece and junctional sarcoplasmic reticulum membrane. As for molecular function, they were associated with ubiquitin-like protein binding, GTPase activator activity, estrogen receptor binding, intermediate filament binding, inorganic anion exchanger activity and cation binding.

Further KEGG pathway analysis found significantly enriched pathways with the top ten enrichment scores [$-\log_{10}(P\text{-value})$] (Fig. 4). Epstein-Barr virus infection, phagosome, human T lymphotropic virus type I infection, viral myocarditis, allograft rejection, graft-versus-host disease, type 1 diabetes mellitus, cellular senescence, endocytosis, and valine, leucine and isoleucine degradation were included in the top ten pathways of the up-regulated circRNAs. Of these pathways, the Epstein-Barr virus infection had the highest enrichment score. On the other hand, the top six pathways of down-regulated circRNAs were proximal tubule bicarbonate reclamation, pancreatic secretion, vascular smooth muscle contraction, focal adhesion, insulin

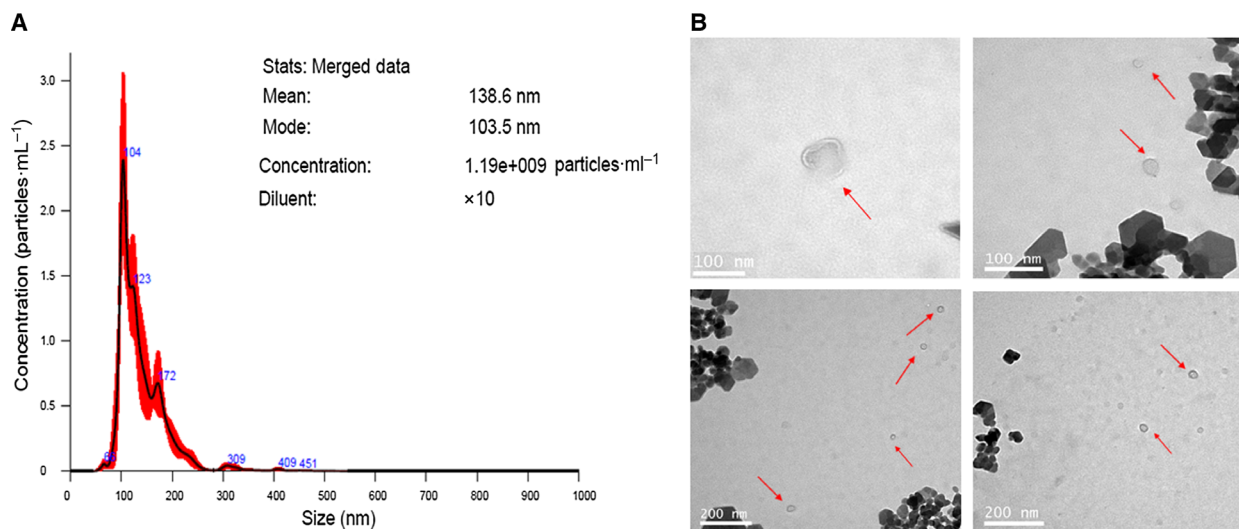


Fig. 1. Detection of EVs isolated from human plasma. (A) Vesicle size distribution of one representative EV was measured by NTA. The mean is the average size of all vesicles measured, and the mode means the size of vesicles that occurred most frequently, that is, the size of the vesicles at the peak. (B) Representative images of EVs. Morphology of the EVs was determined by TEM. Scale bars, 100 nm (top panels); 200 nm (lower panels).

Table 2. Top 30 differentially expressed circRNAs in pancreatic cancer. FC, fold change; FDR, false discovery rate.

circBaseID	logFC	P-value	FDR	Regulation	Catalog	Chromosome	Strand	Gene name
hsa_circ_0002130	6.2167151	1.642E-5	0.0478168	Up	Exonic	chr19	-	C3
hsa_circ_0000896	5.6680874	0.0001058	0.1491639	Up	Exonic	chr19	-	FARSA
hsa_circ_0101692	5.6180826	0.0001281	0.1621948	Up	Sense overlapping	chr14	-	EGLN3
hsa_circ_0005882	5.4368493	4.975E-5	0.1034647	Up	Exonic	chr2	-	STK39
hsa_circ_0001250	5.0584905	0.0008941	0.3949192	Up	Exonic	chr22	+	GRAMD4
hsa_circ_0037096	4.834883	0.0018159	0.3949192	Up	Exonic	chr15	-	PCSK6
hsa_circ_0000128	4.8122453	0.0019492	0.3949192	Up	Exonic	chr1	+	SCNM1
hsa_circ_0000606	4.7943845	0.0020557	0.3949192	Up	Sense overlapping	chr15	-	ICE2
hsa_circ_0007177	4.7822821	0.0021337	0.3949192	Up	Exonic	chr7	+	CCZ1
hsa_circ_0008590	4.7757813	0.0021697	0.3949192	Up	Exonic	chr19	+	RELB
hsa_circ_0006404	4.7409399	0.0024077	0.3949192	Up	Exonic	chr6	+	FOXO3
hsa_circ_0005552	4.7304015	0.0024841	0.3949192	Up	Exonic	chr2	-	EHBP1
hsa_circ_0008615	4.7262769	0.0025109	0.3949192	Up	Exonic	chr19	+	PPP1R13L
hsa_circ_0074368	4.7229576	0.0025364	0.3949192	Up	Exonic	chr5	+	ARHGAP26
hsa_circ_0001821	4.7214258	0.002551	0.3949192	Up	Exonic	chr8	+	PVT1
hsa_circ_0103896	-4.353607	0.0045003	0.3949192	Down	Exonic	chr15	+	G027572
hsa_circ_0006662	-4.306561	0.0052713	0.3949192	Down	Exonic	chr2	+	GLS
hsa_circ_0092763	-4.280169	0.0057533	0.3949192	Down	Exonic	chr10	+	ATRNL1
hsa_circ_0035432	-4.232185	0.0025918	0.3949192	Down	Exonic	chr15	+	CGNL1
hsa_circ_0094190	-4.033311	0.0120721	0.3949192	Down	Exonic	chr10	+	KAT6B
hsa_circ_0013652	-3.937573	0.0157776	0.3949192	Down	Exonic	chr1	-	CSDE1
hsa_circ_0119741	-3.895892	0.0178304	0.3949192	Down	Exonic	chr2	+	LCLAT1
hsa_circ_0091122	-3.824523	0.0214853	0.3949192	Down	Exonic	chrX	+	ATP7A
hsa_circ_0042341	-3.738547	0.0274489	0.3949192	Down	Exonic	chr17	-	SHMT1
hsa_circ_0138455	-3.683197	0.0330624	0.3949192	Down	Exonic	chr9	+	FOCAD
hsa_circ_0130728	-3.630147	0.0379107	0.3949192	Down	Exonic	chr6	-	MOXD1
hsa_circ_0091682	-3.612208	0.0396748	0.3949192	Down	Exonic	chrX	+	MTM1
hsa_circ_0008678	-3.570223	0.0451113	0.3949192	Down	Exonic	chr9	+	FOCAD
hsa_circ_0116742	-3.539399	0.0475604	0.3949192	Down	Exonic	chr22	-	EFCAB6
hsa_circ_0019985	-3.539399	0.0475604	0.3949192	Down	Exonic	chr10	-	SORCS1

secretion and miRNAs in cancer. The proximal tubule bicarbonate reclamation had the highest enrichment score among these signaling pathways.

Validation of the accuracy of the circRNA-seq data

According to the ranking order of the magnitude of fold changes and *P*-values of the differentially expressed circRNAs, five down-regulated circRNAs and eight up-regulated circRNAs were selected (Table 2), and quantitative real-time PCR analysis was performed to confirm the expression profiles of these circRNAs (Fig. 5). The results indicated that 10 out of 13 circRNAs ($P < 0.05$) showed the same change trends and statistical significance as the circRNA-seq data. These findings demonstrated that the circRNA expression profiles obtained from RNA-seq were

consistent with the results of quantitative real-time PCR analysis.

Furthermore, to demonstrate that the EVs circRNAs mentioned earlier were derived from pancreatic cancer, four up-regulated circRNAs selected from Table 2 were validated by quantitative real-time PCR analysis using four human PC cell lines. On the basis of the results, these selected circRNAs all expressed in PC cell lines, especially *has_circ_0000896* and *has_circ_0000128* remarkably expressed in SW1990 compared with other cell lines. Further research will be carried out to identify their role in the development of pancreatic cancer.

Construction of the circRNA-miRNA interaction network

It has been well known that circRNAs play a key role as miRNA sponges to regulate the expression levels of

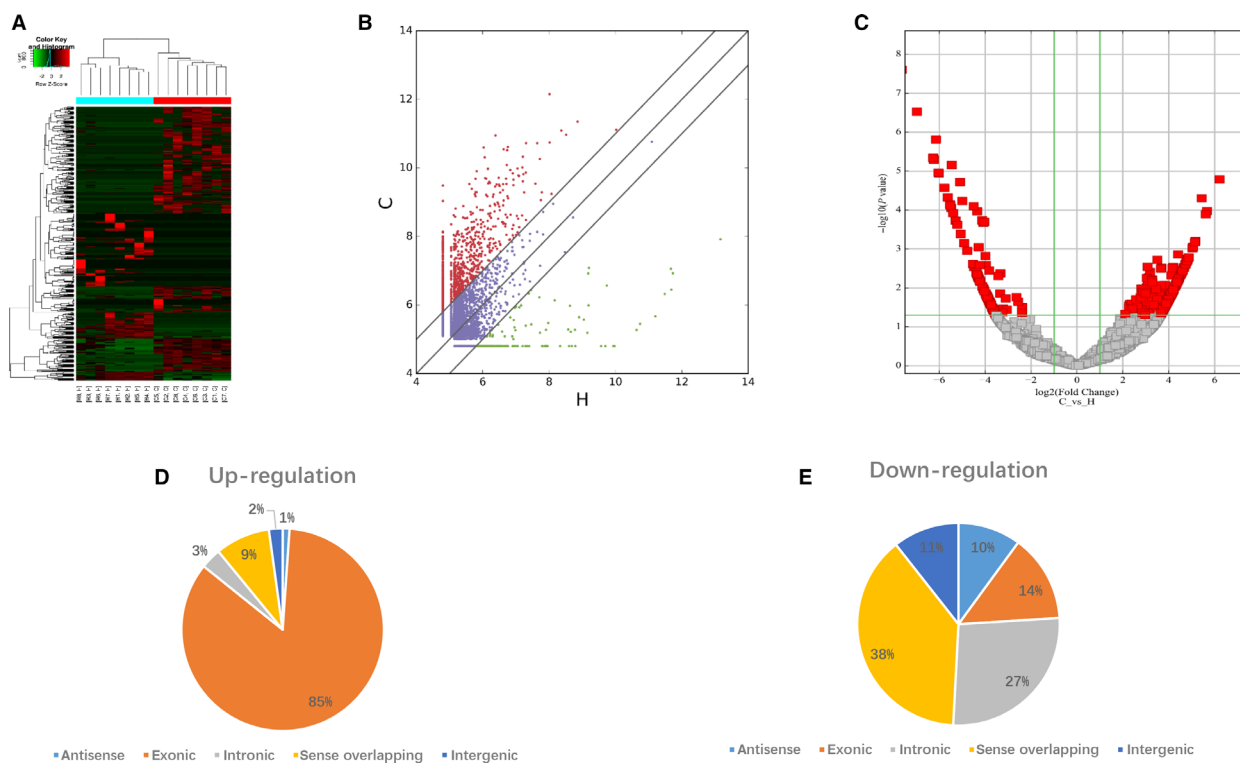


Fig. 2. Differential expression of circRNAs in EVs between patients with PDAC and healthy volunteers. (A) Heatmap for the 453 significant differentially expressed circRNAs between EVs of PDAC and normal control. C1–C8 represent samples from patients with PDAC, and H1–H8 represent samples from healthy controls. Each row represents a circRNA, and each column represents a sample. Hierarchical clustering analysis of the samples was shown. (B) The scatterplot showed the EVs circRNA expression variation between patients with PDAC and healthy control subjects. The values of the x and y axes in the scatterplot are the averaged normalized signal values of groups of samples (log₂ scaled). The oblique lines are fold change lines. The circRNAs above the top oblique line and below the bottom oblique line indicated more than 2-fold change of circRNAs between the two groups of samples. (C) Volcano plot of the differentially expressed circRNAs. The vertical lines demark the fold change values, whereas the green horizontal line marks a *P*-value of 0.05. The red squares in the plot represent the differentially expressed circRNAs in patients with PDAC compared with the control subjects ($P < 0.05$), corresponding to 2-fold up and down, respectively. (D, E) Classification of the dysregulated circRNAs by a pie chart.

other related RNAs by miRNA response elements. Therefore, we tried to identify the interaction of circRNAs and miRNAs in the next step. To theoretically predict miRNA binding sites of the circRNAs, we used miRanda and Target Scan database for conserved seed-matching sequencing, and the 13 validated circRNAs were selected to construct the circRNA-miRNA network using CYTOSCAPE software (Fig. 6). The network showed that hsa-miR-619-5p, hsa-miR-6825-5p, hsa-miR-3916, hsa-miR-6756-5p and hsa-

miR-4739, hsa-miR-6779-5p, hsa-miR-6797-5p and hsa-miR-6812-5p were regulated by a greater number of circRNAs than other miRNAs.

Discussion

Because of its important role in communicating with the tumor microenvironment, EVs have been widely reported in tumor research. In recent years, scientists have found that circulating EVs could be used as a potential

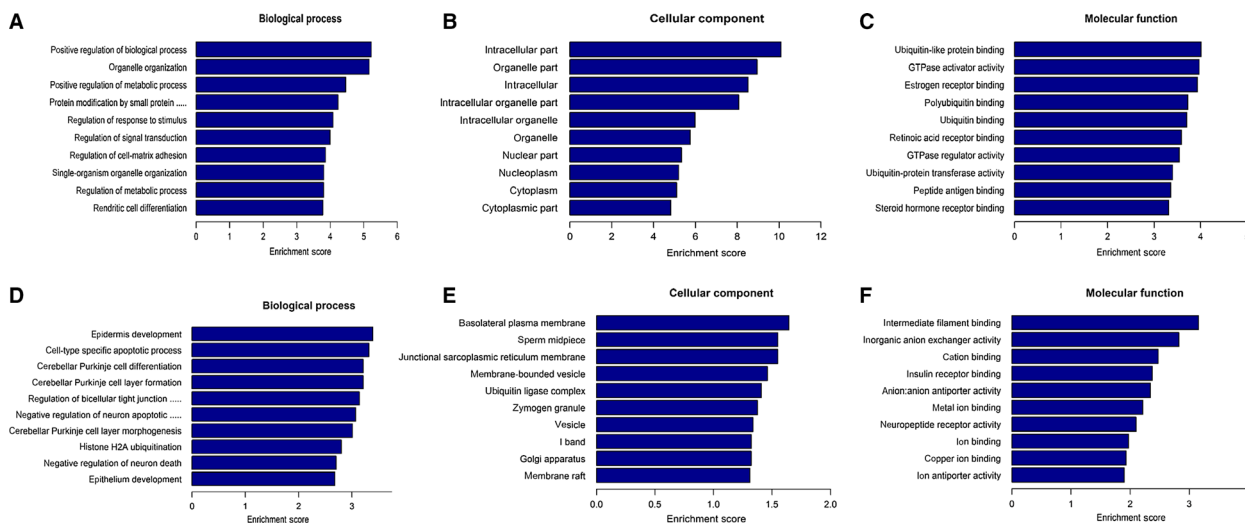


Fig. 3. GO analysis of the dysregulated EVs circRNAs in patients with PDAC. The horizontal axis represents the enrichment scores for the GO terms, and each column represents a GO term. (A–C) GO analysis of the up-regulated circRNAs was shown in terms of (A) BP, (B) CC and (C) molecular function, respectively. (D–F) GO analysis of the down-regulated circRNAs was shown in terms of (D) BP, (E) CC and (F) molecular function, respectively.

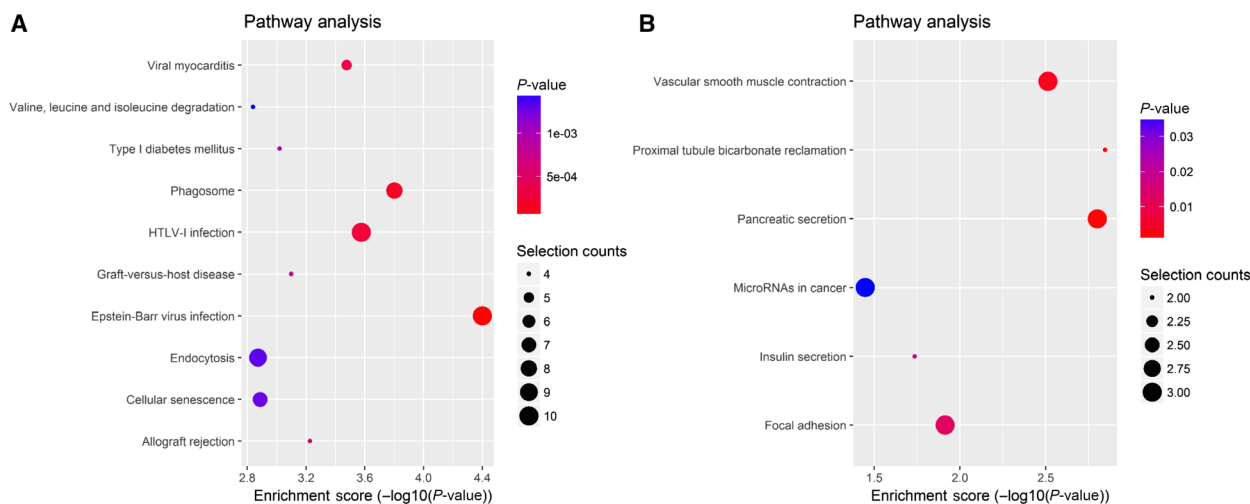


Fig. 4. KEGG pathway analysis of the dysregulated EVs circRNAs in patients with PDAC. (A) Top ten annotated significant pathways of the up-regulated circRNAs were shown. (B) Top six annotated significant pathways of the down-regulated circRNAs were shown. The horizontal axis is the $-\log P$ (logarithm of P -value) for the pathway, and the vertical axis is the pathway category. $P < 0.05$ was considered significant.

biomarker for the diagnosis of PDAC [31,32], but the molecular basis on which PDAC-derived EVs regulate the development of PDAC requires further clarification. Herein, we delineated for the first time the expression profiles of the circRNAs derived from EVs of patients with PDAC by high-throughput whole transcriptome sequencing and following bioinformatic analyses.

First, we isolated EVs from the plasma of eight patients with PDAC and eight healthy volunteers using the ultracentrifugation method. The collected EVs were subsequently detected by NTA and TEM analyses, and the results confirmed the size and form of these EVs.

In the next step, circRNAs from the isolated EVs were sequenced, and we found that 453 circRNAs were significantly differentially expressed in patients with PDAC compared with the healthy control subjects, including 274 up-regulated and 179 down-regulated. To verify the circRNA-seq data, we selected the top 13 differentially expressed circRNAs on the basis of the ranking order in Table 2 to conduct quantitative real-time PCR analysis, and the results confirmed the accuracy of the circRNA-seq data. To demonstrate that these circRNAs were derived from pancreatic cancer, the expressions of four up-regulated circRNAs in PC cell lines were also validated by quantitative real-time PCR analysis. Given that the release of EVs is an important mechanism for tumor cells to communicate with the tumor microenvironment, these differentially expressed circRNAs may participate in the development of PDAC as key content of EVs.

Further GO analysis was performed to explore the potential function of these circRNAs. The data of GO

analysis indicated that these circRNAs are strongly associated with a series of biological activities and metabolic processes in terms of BPs. In regard to CCs, they exhibited a strong relationship with intracellular part, organelle part and so on. As for MPs, they showed capacities to bind with specific proteins, GTPase activator activity and so on. Therefore, the functional roles of these differentially expressed circRNAs are possibly associated with normal cell activities and signal transduction.

In addition, results of the KEGG pathway analysis indicated that differentially expressed circRNAs mainly participate in several biological pathways, such as Epstein-Barr virus infection and miRNAs in cancer. Of these pathways, the most relevant pathway is Epstein-Barr virus infection, which is the first herpesvirus identified to be associated with a remarkably diverse range of cancer types, such as lymphoma, nasopharyngeal cancer, gastric cancer and breast cancer [33–37]. However, its relationship with PDAC remains unclear yet. miRNAs in cancer have been a hot area of cancer research for several years, and many miRNAs are found dysregulated in different cancer types. By targeting mRNAs, miRNAs could influence a lot of cancer-related processes such as cell growth, migration, apoptosis and metabolism [38]. Because circRNAs can function as miRNA sponges to modulate miRNA activity, and considering that EVs are key players in intercellular communication between tumor cells and their microenvironment, we suspected that the differentially expressed circRNAs we identified might affect PDAC progression and cell transformation by targeting miRNAs after release from EVs. On

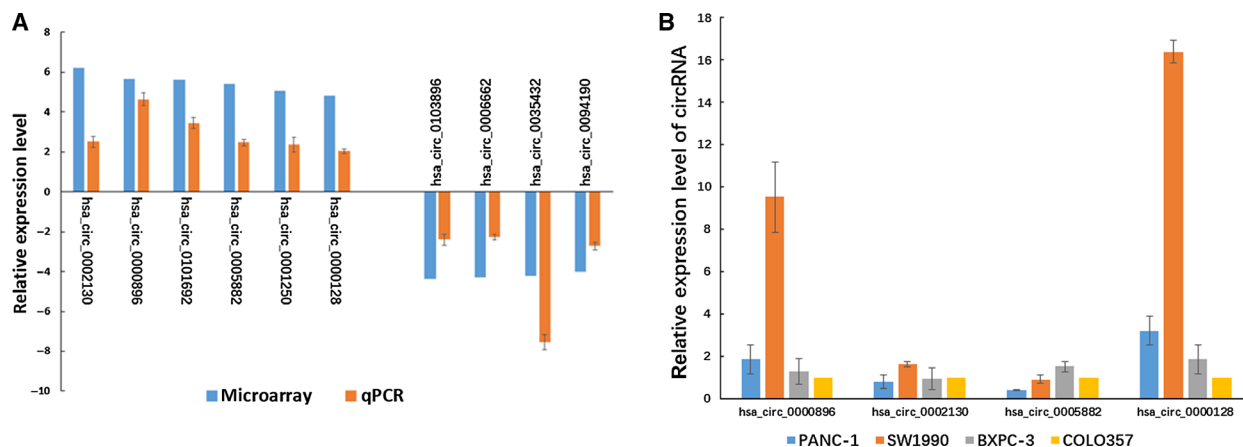


Fig. 5. (A) Validation of the differentially expressed circRNAs obtained from circRNA-seq data. The expression of the top eight up-regulated and top five down-regulated circRNAs obtained from RNA-seq was validated by quantitative real-time PCR analysis using EVs of 14 patients with PDAC and healthy control subjects. (B) Expression levels of four up-regulated circRNAs were detected in four kinds of human pancreatic cancer cell lines. The y axis is the log₂-transformed median fold changes in expression, and data were presented as the mean and standard deviation values. These experiments were repeated three times.

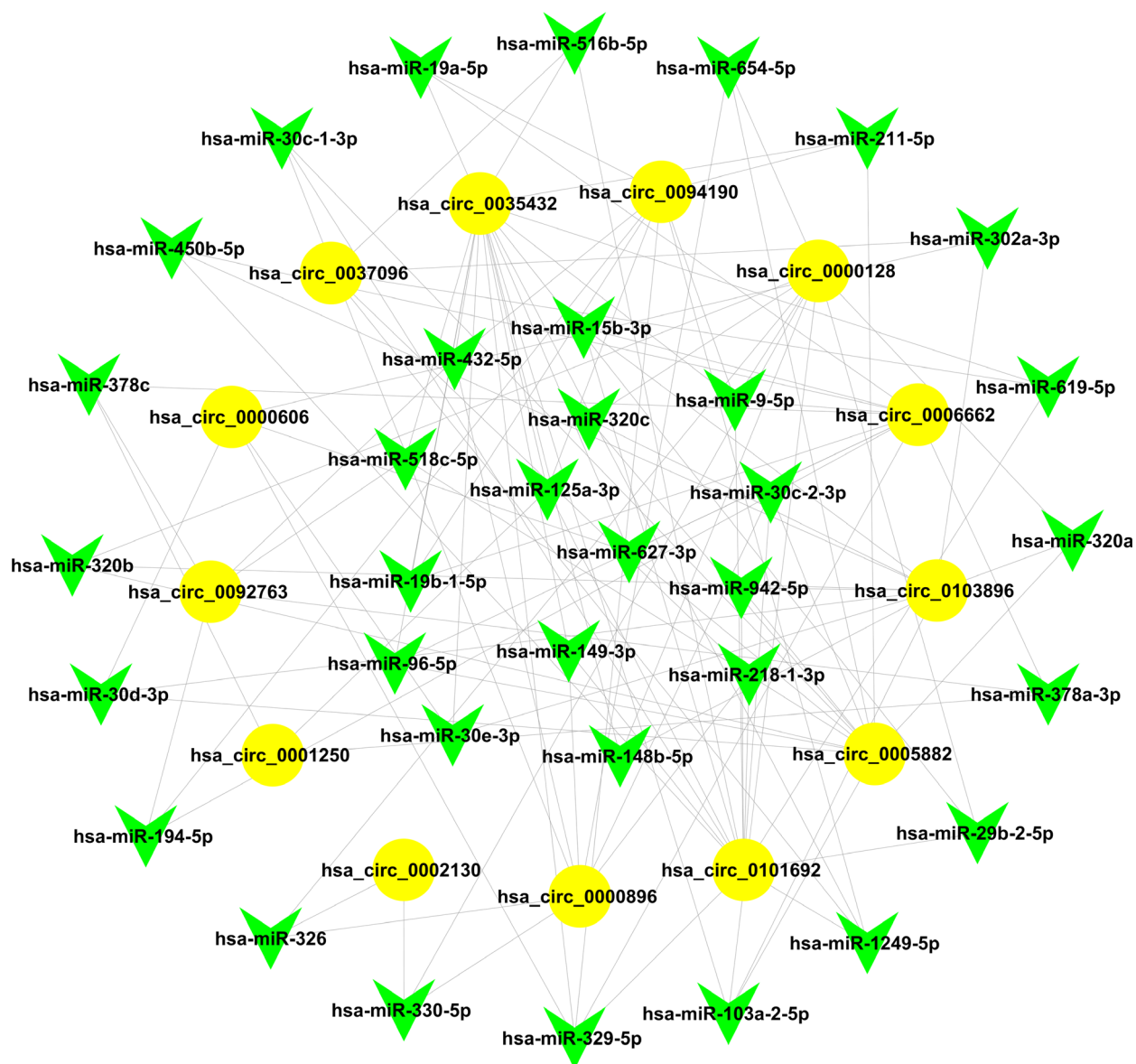


Fig. 6. Predicted circRNA-miRNA interaction network of the 13 selected differentially expressed circRNAs. Yellow cycles represent circRNAs, and green arrows represent miRNAs.

the basis of KEGG pathway analysis, we hypothesized that these circRNAs possibly regulated PDAC progression through one or some of these pathways. However, all of our hypotheses need further verification.

In addition, the interaction between the 13 selected circRNAs and their miRNA targets were predicted by conserved seed-matching sequencing using TargetScan and miRanda database, and a network was constructed by CYTOSCAPE software. The circRNA-miRNA network indicated that all of the differentially expressed circRNAs have their respective miR

response elements, and these data will provide direction for further studies.

In summary, the present work, for the first time, identified a series of differentially expressed circRNAs derived from EVs of patients with PDAC compared with healthy controls. GO and KEGG pathway analyses indicated potential functional roles of these circRNAs in humans, and a circRNA-miRNA interaction network was graphed according to our predictions. Our data link EVs, circRNAs and miRNAs in PDAC together, which will provide novel targets

for further studies about mechanisms of PDAC progression and therapeutic strategies against PDAC.

Acknowledgements

This work was supported by grants from Important Weak Subject Construction Project of Pudong Health and Family Planning Commission of Shanghai (grant no. PWZbr2017-06) and Scientific Research Project of Shanghai Municipal Health and Family Planning Commission (grant no. 20184Y0213).

Conflict of interest

The authors declare no conflict of interest.

Author contributions

HJ and YDL planned experiments. QL, SG, HY and YL performed experiments. SZ and LP analyzed data. QL, JG and XN wrote the manuscript. All authors edited and approved the final version of the manuscript.

References

- 1 Siegel RL, Miller KD and Jemal A (2019) Cancer statistics, 2019. *CA Cancer J Clin* **69**, 7–34.
- 2 de Sousa Cavalcante L and Monteiro G (2014) Gemcitabine: metabolism and molecular mechanisms of action, sensitivity and chemoresistance in pancreatic cancer. *Eur J Pharmacol* **741**, 8–16.
- 3 Johnstone RM, Adam M, Hammond JR, Orr L and Turbide C (1987) Vesicle formation during reticulocyte maturation. Association of plasma membrane activities with released vesicles (exosomes). *J Biol Chem* **262**, 9412–9420.
- 4 Chen R, Fu M, Zhang G, Zhou Y, Zhu S, Liu J, Wang D, Deng A and Wang Z (2014) Rac1 regulates skin tumors by regulation of keratin 17 through recruitment and interaction with CD11b+Gr1+ cells. *Oncotarget* **5**, 4406–4417.
- 5 Thery C, Zitvogel L and Amigorena S (2002) Exosomes: composition, biogenesis and function. *Nat Rev Immunol* **2**, 569–579.
- 6 Thery C, Boussac M, Veron P, Ricciardi-Castagnoli P, Raposo G, Garin J and Amigorena S (2001) Proteomic analysis of dendritic cell-derived exosomes: a secreted subcellular compartment distinct from apoptotic vesicles. *J Immunol* **166**, 7309–7318.
- 7 Valadi H, Ekstrom K, Bossios A, Sjostrand M, Lee JJ and Lotvall JO (2007) Exosome-mediated transfer of mRNAs and microRNAs is a novel mechanism of genetic exchange between cells. *Nat Cell Biol* **9**, 654–659.
- 8 Raposo G and Stoorvogel W (2013) Extracellular vesicles: exosomes, microvesicles, and friends. *J Cell Biol* **200**, 373–383.
- 9 Denzer K, van Eijk M, Kleijmeer MJ, Jakobson E, de Groot C and Geuze HJ (2000) Follicular dendritic cells carry MHC class II-expressing microvesicles at their surface. *J Immunol* **165**, 1259–1265.
- 10 Bang C and Thum T (2012) Exosomes: new players in cell-cell communication. *Int J Biochem Cell Biol* **44**, 2060–2064.
- 11 Chivet M, Hemming F, Pernet-Gallay K, Fraboulet S and Sadoul R (2012) Emerging role of neuronal exosomes in the central nervous system. *Front Physiol* **3**, 145.
- 12 Malm T, Loppi S and Kanninen KM (2016) Exosomes in Alzheimer's disease. *Neurochem Int* **97**, 193–199.
- 13 Skog J, Wurdinger T, van Rijn S, Meijer DH, Gainche L, Sena-Esteves M, Curry WT Jr, Carter BS, Krichevsky AM and Breakefield XO (2008) Glioblastoma microvesicles transport RNA and proteins that promote tumour growth and provide diagnostic biomarkers. *Nat Cell Biol* **10**, 1470–1476.
- 14 Kosaka N, Yoshioka Y, Tominaga N, Hagiwara K, Katsuda T and Ochiya T (2014) Dark side of the exosome: the role of the exosome in cancer metastasis and targeting the exosome as a strategy for cancer therapy. *Future Oncol* **10**, 671–681.
- 15 Melo SA, Luecke LB, Kahler C, Fernandez AF, Gammon ST, Kaye J, LeBleu VS, Mittendorf EA, Weitz J, Rahbari N *et al.* (2015) Glypican-1 identifies cancer exosomes and detects early pancreatic cancer. *Nature* **523**, 177–182.
- 16 Singh R, Pochampally R, Watabe K, Lu Z and Mo YY (2014) Exosome-mediated transfer of miR-10b promotes cell invasion in breast cancer. *Mol Cancer* **13**, 256.
- 17 Zhao ZJ and Shen J (2017) Circular RNA participates in the carcinogenesis and the malignant behavior of cancer. *RNA Biol* **14**, 514–521.
- 18 Qu S, Yang X, Li X, Wang J, Gao Y, Shang R, Sun W, Dou K and Li H (2015) Circular RNA: a new star of noncoding RNAs. *Cancer Lett* **365**, 141–148.
- 19 Li J, Yang J, Zhou P, Le Y, Zhou C, Wang S, Xu D, Lin HK and Gong Z (2015) Circular RNAs in cancer: novel insights into origins, properties, functions and implications. *Am J Cancer Res* **5**, 472–480.
- 20 Ebbesen KK, Hansen TB and Kjems J (2017) Insights into circular RNA biology. *RNA Biol* **14**, 1035–1045.
- 21 Hansen TB, Jensen TI, Clausen BH, Bramsen JB, Finsen B, Damgaard CK and Kjems J (2013) Natural RNA circles function as efficient microRNA sponges. *Nature* **495**, 384–388.
- 22 Memczak S, Jens M, Elefsinioti A, Torti F, Krueger J, Rybak A, Maier L, Mackowiak SD, Gregersen LH, Munschauer M *et al.* (2013) Circular RNAs are a large

- class of animal RNAs with regulatory potency. *Nature* **495**, 333–338.
- 23 Li F, Zhang L, Li W, Deng J, Zheng J, An M, Lu J and Zhou Y (2015) Circular RNA ITCH has inhibitory effect on ESCC by suppressing the Wnt/beta-catenin pathway. *Oncotarget* **6**, 6001–6013.
- 24 Shao Y and Chen Y (2016) Roles of circular RNAs in neurologic disease. *Front Mol Neurosci* **9**, 25.
- 25 Burd CE, Jeck WR, Liu Y, Sanoff HK, Wang Z and Sharpless NE (2010) Expression of linear and novel circular forms of an INK4/ARF-associated non-coding RNA correlates with atherosclerosis risk. *PLoS Genet* **6**, e1001233.
- 26 Hansen TB, Kjems J and Damgaard CK (2013) Circular RNA and miR-7 in cancer. *Can Res* **73**, 5609–5612.
- 27 Li H, Hao X, Wang H, Liu Z, He Y, Pu M, Zhang H, Yu H, Duan J and Qu S (2016) Circular RNA expression profile of pancreatic ductal adenocarcinoma revealed by microarray. *Cell Physiol Biochem* **40**, 1334–1344.
- 28 Zhao J, Li L, Wang Q, Han H, Zhan Q and Xu M (2017) CircRNA expression profile in early-stage lung adenocarcinoma patients. *Cell Physiol Biochem* **44**, 2138–2146.
- 29 Li Y, Zheng Q, Bao C, Li S, Guo W, Zhao J, Chen D, Gu J, He X and Huang S (2015) Circular RNA is enriched and stable in exosomes: a promising biomarker for cancer diagnosis. *Cell Res* **25**, 981–984.
- 30 Kefas B, Godlewski J, Comeau L, Li Y, Abounader R, Hawkinson M, Lee J, Fine H, Chiocca EA, Lawler S *et al.* (2008) microRNA-7 inhibits the epidermal growth factor receptor and the Akt pathway and is down-regulated in glioblastoma. *Can Res* **68**, 3566–3572.
- 31 Lau C, Kim Y, Chia D, Spielmann N, Eibl G, Elashoff D, Wei F, Lin YL, Moro A, Grogan T *et al.* (2013) Role of pancreatic cancer-derived exosomes in salivary biomarker development. *J Biol Chem* **288**, 26888–26897.
- 32 Arscott WT and Camphausen KA (2011) EGFR isoforms in exosomes as a novel method for biomarker discovery in pancreatic cancer. *Biomark Med* **5**, 821.
- 33 Vockerodt M, Yap LF, Shannon-Lowe C, Curley H, Wei W, Vrzalikova K and Murray PG (2015) The Epstein-Barr virus and the pathogenesis of lymphoma. *J Pathol* **235**, 312–322.
- 34 Cohen JI, Fauci AS, Varmus H and Nabel GJ (2011) Epstein-Barr virus: an important vaccine target for cancer prevention. *Sci Transl Med* **3**, 107fs7.
- 35 Tsang CM and Tsao SW (2015) The role of Epstein-Barr virus infection in the pathogenesis of nasopharyngeal carcinoma. *Virology* **30**, 107–121.
- 36 Zhao J, Jin H, Cheung KF, Tong JH, Zhang S, Go MY, Tian L, Kang W, Leung PP, Zeng Z *et al.* (2012) Zinc finger E-box binding factor 1 plays a central role in regulating Epstein-Barr virus (EBV) latent-lytic switch and acts as a therapeutic target in EBV-associated gastric cancer. *Cancer* **118**, 924–936.
- 37 Mazouni C, Fina F, Romain S, Ouafik L, Bonnier P, Brandone JM and Martin PM (2011) Epstein-Barr virus as a marker of biological aggressiveness in breast cancer. *Br J Cancer* **104**, 332–337.
- 38 Hayes J, Peruzzi PP and Lawler S (2014) MicroRNAs in cancer: biomarkers, functions and therapy. *Trends Mol Med* **20**, 460–469.